Common host factors for internal ribosomal entry site-mediated translation of viral genomic RNA: An investigation in foot-and-mouth disease and classical swine fever viruses

Rupaly Akhter [a], Kazi Anowar Hossain [a], Bouchra Kitab [a], Yoshihiro Sakoda [b], Kyoko Tsukiyama-Kohara [a,*]

[a] Transboundary Animal Disease Center, Joint Faculty of Veterinary Medicine, Kagoshima University, Kagoshima 890-0065, Japan
[b] Department of Disease Control, Faculty of Veterinary Medicine, Hokkaido University, Hokkaido 060-0818, Japan

ARTICLE INFO

ABSTRACT

We previously proposed polycystic kidney disease1-like 3 (PKD1L3) and ubiquitin-specific peptidase 31 (USP31) as potential common host factors for IRES-mediated RNA translation in infections with foot-and-mouth disease virus (FMDV) and classical swine fever virus (CSFV). However, those findings required substantiation, and the specific roles of these factors in the IRES-mediated translation remained unclear. Accordingly, in this study, we aimed to confirm the roles of PKD1L3 and USP31 as host factors associated with IRES activity in bi-cistronic reporter assays, and to investigate the interactions of these host proteins during IRES activity. *PKD1L3* and *USP31* silencing suppressed IRES activity in both FMDV and CSFV RNAs. *PKD1L3* and *USP31* overexpression had no significant effects. *PKD1L3* and *USP31* silencing also suppressed viral RNA replication for CSFV and infection with another picornavirus (from the same family as FMDV), encephalomyocarditis virus. Immunoprecipitation assays revealed that PKD1L3 and USP31 can interact with each other. We also examined their interaction with a eukaryotic translation factor involved in the IRES of hepatitis C virus (HCV), eIF3c. PKD1L3 and more pronouncedly USP31 can interact with eIF3c. Immunofluorescent assays revealed partial, cytoplasmic co-localization of USP31 with PKD1L3, eIF3c, and Hsp90β. Moreover, silencing of *eIF3c* and *Hsp90β* suppressed FMDV- and CSFV-IRES activity. Our results indicate the possibility that PKD1L3 and USP31 can participate in IRES activity by interacting with eIF3c and Hsp90β.

1. Introduction

Foot-and-mouth disease virus (FMDV) and classical swine fever virus (CSFV) are both positive sense, single-stranded RNA viruses that act as pathogens of livestock disease, in cloven-hoofed animals in the case of FMDV, and porcine species in the case of CSFV (Jamal and Belsham, 2013). FMDV belongs to the *Picornaviridae* family, and CSFV to the *Flaviviridae* family, and both viruses cause transboundary animal diseases (Food and Agriculture Organization; FAO) and are endemic in many parts of the world (World Organization of Animal Health; WOAH). Even among countries currently regarded as FMDV- or CSFV-free, outbreaks have occurred within recent years, and both FMDV and CSFV are still regarded as potent threats. Thus, there is a need for mitigation strategies against these pathogens, which could include establishing disease-resistant livestock to guard against the possibility of spillovers from wild animal populations. Developing such strategies depends on a detailed knowledge of how these viruses are able to infect their hosts.

Both FMDV and CSFV utilize internal ribosomal entry site (IRES)-mediated translation, rather than canonical, cap-dependent translation in their genomes. They both possess IRES element in the 5′- UTR regions of their genomic RNA to drive viral protein translation (Belsham and Brangwyn, 1990; Grubman and Baxt, 2004; Rijnbrand et al., 1997). FMDV and CSFV can be regarded as representing the wide range of viruses that exploit IRES-mediated translation. As well as belonging to different virus families, they are also regarded as having different IRES types, with FMDV having a Type I IRES (in common with polio and other picornaviruses) (Belsham and Brangwyn, 1990; Grubman and Baxt, 2004; Rijnbrand et al., 1997) and CSFV having a Type IV IRES (a hepatitis C-like IRES) (Jackson and Kaminski, 1995; Tsukiyama-Kohara et al., 1992). Based on higher-order structures, IRESes can be classified

* Corresponding author.
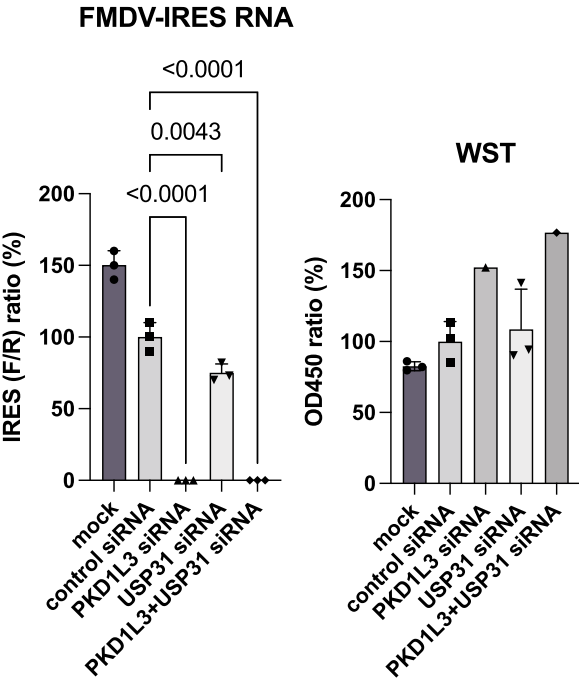*E-mail address:* kkohara@vet.kagoshima-u.ac.jp (K. Tsukiyama-Kohara).

A

FMDV-IRES RNA

WST

B

CSFV-IRES RNA

WST

C

PKD1L3 mRNA

USP31 mRNA
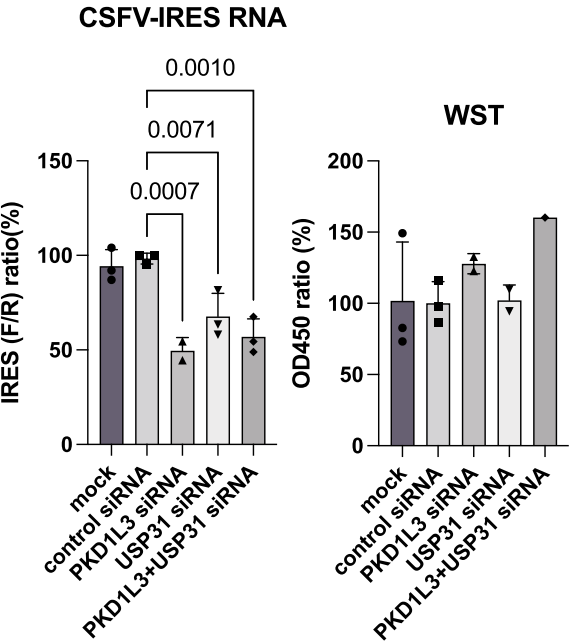
(caption on next page)

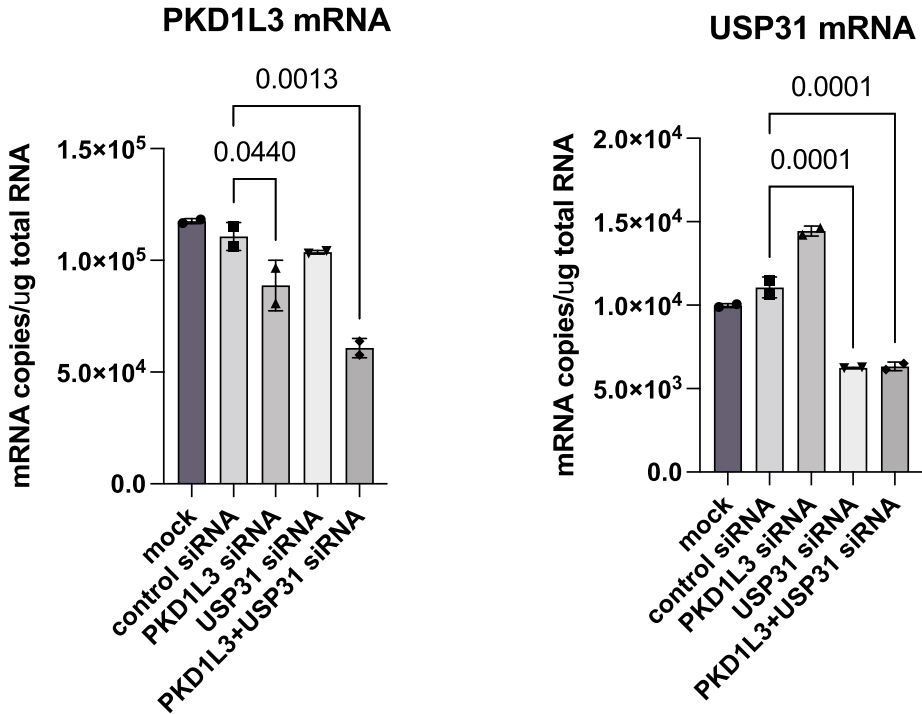**Fig. 1.** Silencing-based assessment of *PKD1L3* and *USP31* using specific siRNAs, and their potential effect on FMDV- and CSFV-IRES activities. **A**. The bi-cistronic FMDV-IRES RNA and *PKD1L3, USP31*, or control siRNA, or subject to mock-transfection, and IRES activity was calculated as the percentage of firefly luciferase (F)/*Renilla* luciferase (R) versus the value for the control siRNA-treated cells (left). The viability of the siRNA-treated cells was determined in a WST-1 assay (right); results for each transfection type are indicated as the percentage of OD_{450} value versus that for control siRNA-treated cells. Vertical bars represent SD. (**B**) The bi-cistronic CSFV-IRES RNA and *PKD1L3, USP31*, or control siRNA, or subject to mock-transfection, and IRES activity was calculated as the percentage of firefly luciferase (F)/*Renilla* luciferase (R) versus the value for the control siRNA-treated cells (left). The viability of the siRNA-treated cells was measured using the WST-1 assay (right). The percentage of OD_{450} value of each siRNA-treated cell when compared with the control siRNA-treated cells is indicated. Vertical bars represent SD. The *p*-value of a significant effect <0.05 is indicated (**C**) Quantitation of *PKD1L3* (left) and *USP31* (right) mRNAs in siRNA-treated cells by RT-qPCR. *P*-values < 0.05 were regarded as significant.

into one of five groups: Group I (PV), II (FMDV), III (hepatitis A virus), IV (HCV-like), or V (Aichi virus-like) (Lozano and Martinez-Salas, 2015). IRES sequences appear to be conserved across a range of viral strains, and thus represent therapeutic targets in drug developmental research (Matsui et al., 2019), where common targets identified for FMDV and CSFV could also be targeted in treatment strategies for other viruses with different IRES types, including poliovirus, encephalomyocarditis virus (EMCV), bovine viral diarrhea virus, and HCV, etc.

We previously identified two common factors potentially involved in IRES-mediated translation for both FMDV and CSFV; specifically, poly-cystic kidney disease1-like 3 (PKD1L3) and ubiquitin-specific peptidase 31 (USP31); both *PKD1L3* and *USP31* were downregulated in recombi-nant FMVD- and CSFV-transfected cells treated with the anti-viral agent pycnogenol®, and IRES activity was abolished when they were silenced (Ide et al., 2022). However, in that study we were unable to make a definite conclusion, because we could not exclude the possibility of a cryptic promoter within the plasmid having an adverse effect on IRES activity measurement. Furthermore, although we identified a possible link between these common host factors and IRES-mediated translation, their exact roles in the infection mechanism and the interactions be-tween them remain unelucidated, which were examined in dengue virus (DENV) infection (Hossain et al., 2024).

Accordingly, in the preset study, we aimed to substantiate the links between PKD1L3 and USP31 and FMDV- and CSFV IRES-mediated translation using bi-cistronic RNA reporters, and to investigate in-teractions between the host factors in immunoprecipitation assays and the effects of the relevant RNA silencing on FMDV- and CSFV-IRES activities.

2. Materials and methods

2.1. Cells

Human embryonic kidney cell lines (HEK293, B10, and pCI5) were cultured as described previously (Matsui et al., 2019). HEK293 cells had been purchased from the American Type Culture Collection (ATCC, HEK293T/17, CRL-11,268), and we used them to establish dedicated cell lines for bicistronic vector-based FMDV (B10 line) and CSFV (pCI5 line) IRES activity assessments (Supplementary Figs. S1A, B), as described previously for FMDV (Matsui et al., 2019) and CSFV (Ide et al., 2022). These cells were maintained in Dulbecco's modified Eagle's medium (DMEM; Nissui, Tokyo, Japan) supplemented with 10 % fetal calf serum (FCS; Bovogen Pty Ltd., Australia) and glutamine. All cell lines were cultured at 37 °C in a 5 % CO_2 atmosphere.

2.2. IRES-expressing bi-cistronic vectors

We constructed bi-cistronic vectors containing IRES sequences be-tween the *Renilla* and firefly luciferase genes using a pCAGGS-Neo expression vector system (Supplementary Fig. S1, Matsui et al., 2019). Specifically, our bi-cistronic RNA transcription involved *Renilla* and firefly luciferase genes that straddled the FMDV- or CSFV-IRES, a pRF-FMDV-IRES, or a pRF-CSFV-IRES sequence, to form a vector which also possessed T7 promoters (Supplementary Fig. S2). Bi-cistronic re-porter assays are instrumental in the study of transgene expression, understanding IRES translation, and identification of novel

cap-independent translational elements (van den Akker et al., 2021). In relevant bi-cistronic assays, the IRES sequence is flanked by two reporter genes and expressed downstream of the second cistron. The first cistron represents cap-dependent translation, and the second cistron represents IRES-mediated translation. Thus, the yield ratio of the second cistron versus the first citron represents the standard IRES activity (Jang et al., 1989; Kanda et al., 2016; Matsui et al., 2019). We used a dual luciferase reporter assay (Promega, Madison, WI, USA), which enabled serial measurement of firefly luciferase (F-Luc., second cistron) expression and *Renilla* luciferase (R-Luc., first cistron) expression, in accordance with the manufacturer's protocol. Cells were transfected with plasmid DNAs or RNAs containing bi-cistronic FMDV-IRES or CSFV-IRES constructs, and *PKD1L3* and *USP31*, or control siRNA, or subject to mock-transfection. IRES activity was calculated as the yield ratio of F-Luc./R-luc., and the percentage of expression versus that of control siRNA-treated cells was also calculated for each cistron. The FMDV-IRES (serotype C) sequence (Licursi et al., 2012) was a generous gift from Dr. Kensuke Hirasawa of the Memorial University of Newfoundland. The CSFV-IRES sequence was a generous gift from Professor Graham J. Belsham of the University of Copenhagen.

2.3. Plasmid transfection and assays

Transfection of plasmid DNAs (Fig. 2A, B) into cells was performed using Lipofectamine™ LTX Reagent (Thermo Fisher Scientific Inc., Waltham, MA, USA). Cell viability was evaluated using the water-soluble tetrazolium salt-1 (WST-1) assay (cat# MK400, Takara Bio., Shiga, Japan) with determination of optical density at 450 nm (OD_{450}) in accordance with the manufacturer's instructions. The principle of this assay involves cleavage of the tetrazolium salt (WST-1) to formazan dye, by the succinate-tetrazolium reductase (EC 1.3.99.1) present in the mitochondrial respiratory chain of viable cells; the greater the number of viable cells, the greater the overall mitochondrial dehydrogenase activity, and the greater the production of formazan dye, which thus shows a linear correlation with the number of metabolically active cells in the sample medium. In brief, cells were seeded in 96-well microtiter plates at a density of 5×10^3 cells per well in 100 μl medium. Trans-fected cells were then incubated at 37 °C in a 5 % CO_2 atmosphere for 72 hrs. 10 μl of WST-1 reagent was added to each well and cells were incubated for a further hour at 37 °C in a 5 % CO_2 atmosphere. The OD_{450} was measured, and results were calculated as the percentage of the OD_{450} value for each cell type versus that for the relevant mock-transfected or control siRNA-treated cells. Luciferase assays were per-formed using a dual-luciferase reporter assay system (Promega, Madi-son, WI, USA). Luminescence was measured using a plate-reading luminometer (EnVision 2104, multi-reader; Perkin Elmer Co., MA, USA), as described previously (Kanda et al., 2016). IRES activity was calculated by dividing the firefly luciferase activity by the *Renilla* luciferase (F/R) activity. Results are indicated as the percentage of each value versus that for the relevant control siRNA or mock-transfected cells.

2.4. siRNA, RNA synthesis and transfection, and mRNA quantitation

PKD1L3- and *USP31*-targeting siRNAs were designed using the BLOCK-iT DNAi Designer (Thermo Fisher Scientific Inc.), as described
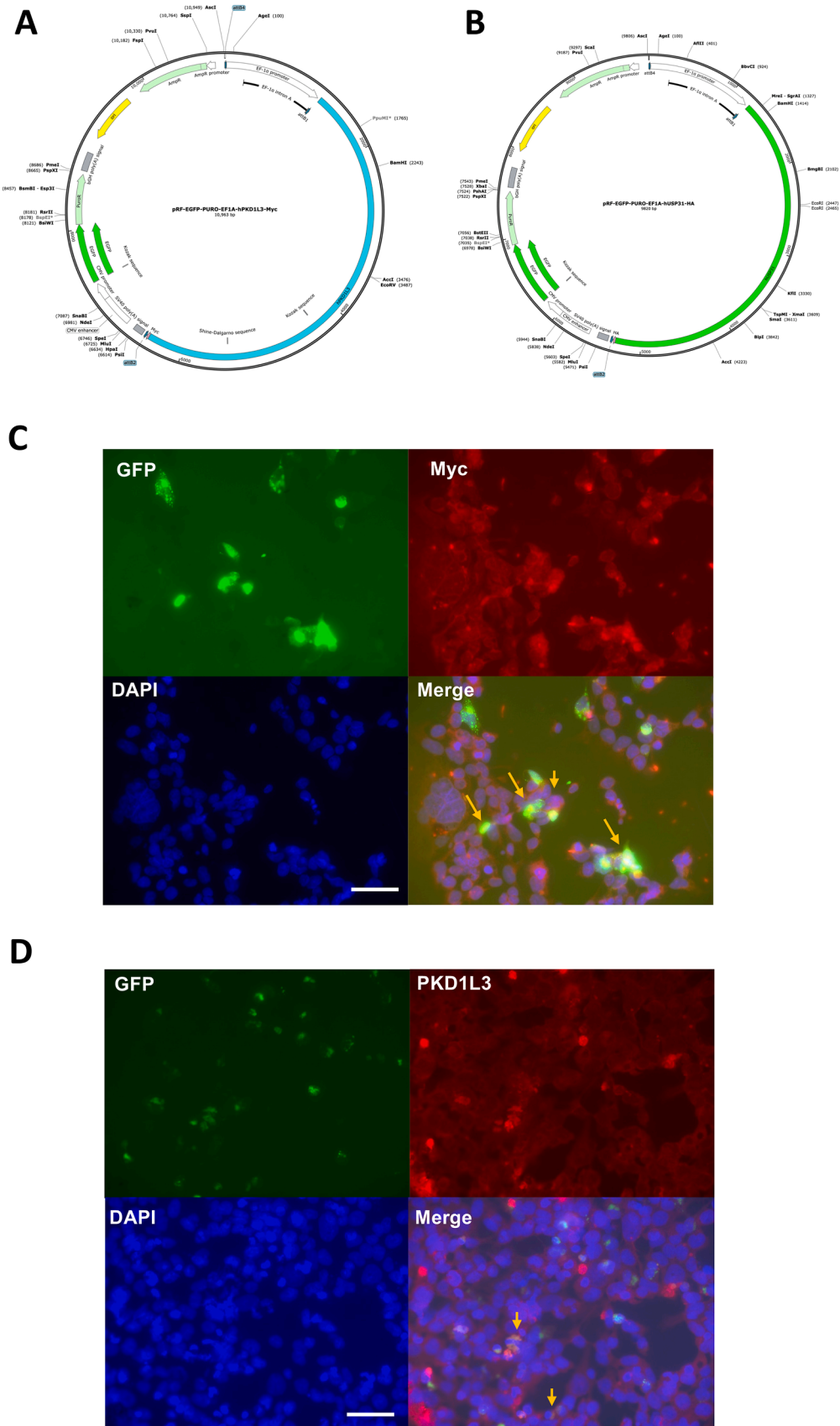
Fig. 2. PKD1L3 and USP31 expression vector structures and their expression level in HEK293 cells examined by IFA. (**A**) Structure of pRF-EGFP-PURO-EF1A-hPKD1L3-Myc plasmid DNA. (**B**) Structure of pRF-EGFP-PURO-EF1A-hUSP31-HA plasmid DNA. (**C, D**) The pRF-EGFP-PURO-EF1A-hPKD1L3-Myc plasmid was transfected into cells and detected through EGFP expression, anti-Myc Ab and anti-mouse Alexa 568 (**C**) or anti-PKD1L3 Ab and anti-rabbit Alexa 568 (**D**) and DAPI staining for the nucleus using a fluorescent microscope BZ-X700 (Keyence Co., Japan). Merged images are also shown (on the right lower side, yellow arrows). Scale bars indicate 50 μm. (**E, F**) The pRF-EGFP-PURO-EF1A-hUSP31-HA plasmid was transfected and detected using GFP expression, anti-HA Ab, and anti-rabbit Alexa

568 staining (**E**) or anti-USP31 Ab, and anti-mouse Alexa 568 staining (**F**), and DAPI staining using a fluorescent microscope. Merged images are also shown (on the right lower side, yellow arrows). Scale bars indicate 50 μm. (**G**) The cells transfected by plasmid vector control were reacted with normal mouse or rabbit IgG. Merged images are shown on the right lower side. Scale bars indicate 50 μm.
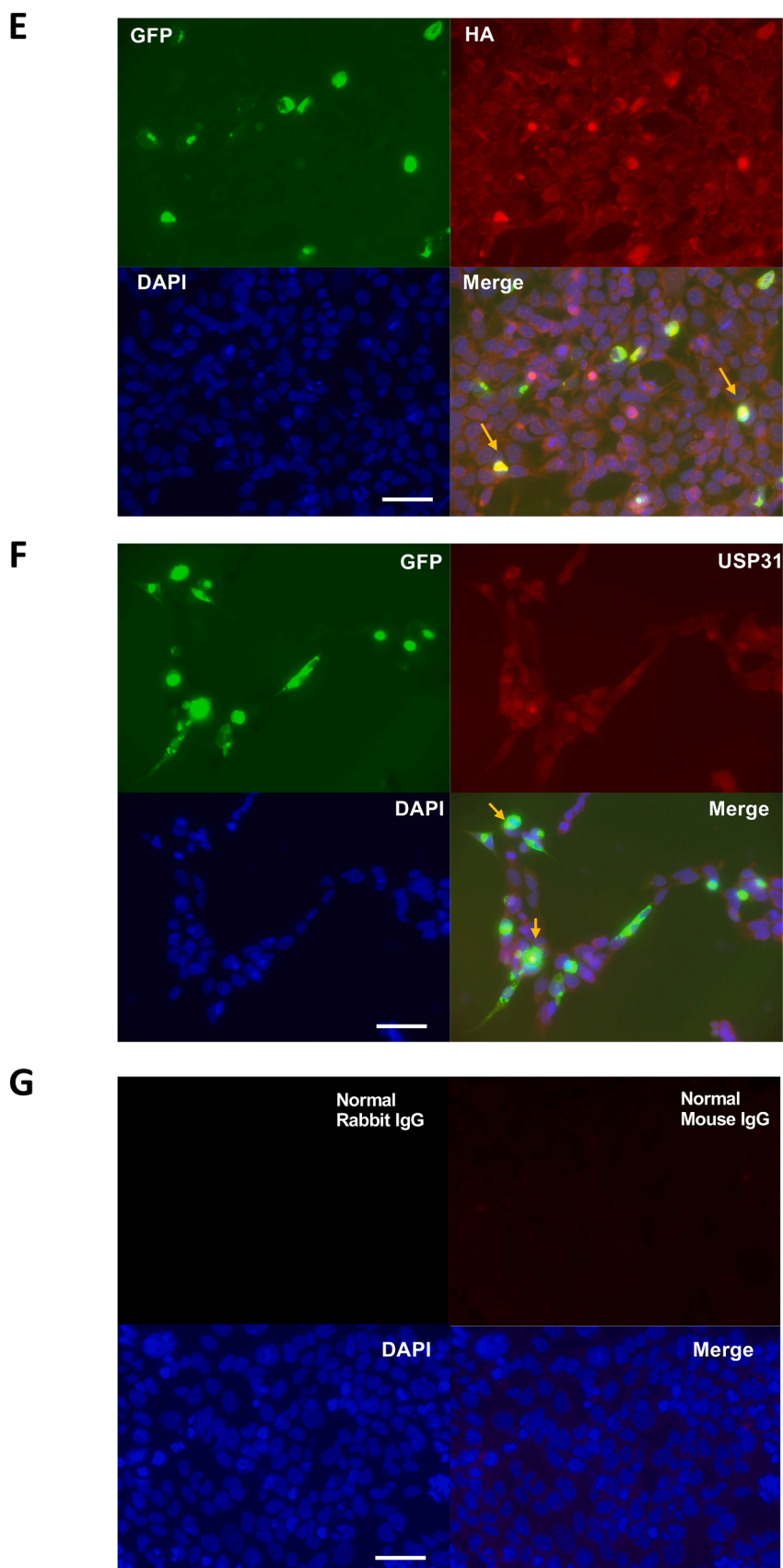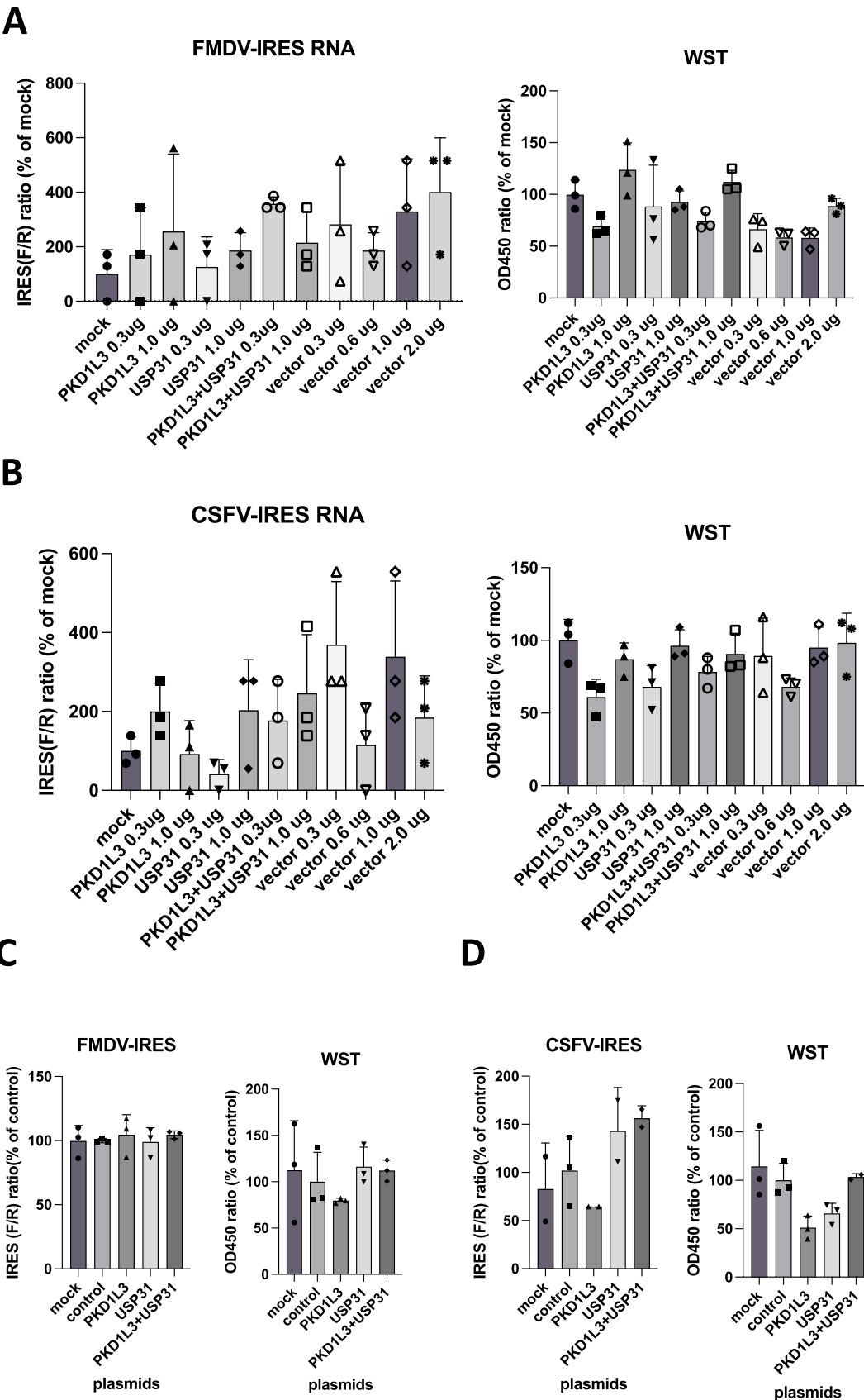

Fig. 2. (*continued*).

A

B

C

D

(caption on next page)

Fig. 3. Effects of PKD1L3 and USP31 overexpression on FMDV- and CSFV- activities. (**A**) HEK293 cells transfected with bi-cistronic FMDV-IRES reporter RNAs (0.5 mg/well) or subject to mock-transfection, or transfected with 0.3, 1.0 mg of plasmid DNAs (pRF-EGFP-PURO-EF1A-hPKD1L3-Myc, pRF-EGFP-PURO-EF1A-hUSP31-HA and vector) singly or in combination. IRES activity was measured using a dual luciferase assay kit and the ratio of F/R was calculated. The percentage of the F/R ratio (%) versus that obtained with mock transfection was calculated (left). Cell viability was determined in a WST-1 assay and the ratio (%) of OD_{450} to mock-treated cells was calculated (right). Vertical bars indicate S.D. (**B**) HEK293 cells transfected with bi-cistronic CSFV-IRES reporter RNAs (0.5 mg/well) were also mock-transfected or transfected with 0.3, 1.0 mg of plasmid DNAs (pRF-EGFP-PURO-EF1A-hPKD1L3-Myc, pRF-EGFP-PURO-EF1A-hUSP31-HA and vector) alone or together. IRES activity was measured using a dual luciferase assay kit and the ratio of F/R was calculated. The percentage of the F/R ratio (%) of the mock was calculated (left). Cell viability was measured by WST assay, and the result is indicated as the percentage (%) of OD_{450} value versus that obtained with mock transfection (right). Vertical bars indicate S.D. (**C**) PKD1L3 was overexpressed by transfection of pRF-EGFP-PURO-EF1A-hPKD1L3-Myc plasmid DNA, USP31 by transfection of pRF-EGFP-PURO-EF1A-hUSP31-HA plasmid DNA or both, vector control and mock in B10 cells. FMDV-IRES activity measured by dual luciferase assay (left) and cell viability measured by WST-1 assay (right) were calculated compared to the control vector transfected cells. The percentage of F/R or OD_{450} value of each cell compared to the control vector transfected cells is indicated. (**D**) CSFV-IRES activity was measured in pCI5 cells overexpressing PKD1L3, USP31, or both, or control vector, and mock-transfected pCI5 cells by dual luciferase assay (left). Cell viability was measured by WST-1 assay (right). These data were calculated as a ratio to the control vector transfected cell values. Vertical bars represent SD. The percentage of F/R or OD_{450} compared to the control siRNA-treated cells is indicated.

previously (Ide et al., 2022). The siRNA sequences were as follows: *PKD1L3* siRNA, 5′-CAGUUCAUGGUUUGCAAGCUCUUAA-3′; *USP31* siRNA, 5′- CAGCACAGCCGCGACUUCAAGACUA-3′. ON-target plus siRNA control (Horizon/Dharmacon, Lafayette, CO, USA) was applied as the control siRNA. Mock transfection was performed without siRNA. These siRNAs (5 nM) were reverse-transfected using Lipofectamine™ RNAiMax Reagent (Invitrogen) following the manufacturer's protocol. Silencing effects were confirmed using RT-qPCR, as described previously (Ide et al., 2022). The *eIF3c*- and *Hsp90β*-targeting siRNAs were purchased from Santa Cruz Biotechnology (Texas, USA). These siRNAs (5 nM) were transfected into cells using Lipofectamine 2000 (Thermo Fisher Scientific Inc.), as described previously (Ujino et al., 2012). pRF-FMDV-IRES and pRF-CSF-IRES RNAs were synthesized using *Hpa*I digested plasmid DNA (Supplementary Fig.S2) using RiboMax large scale RNA production systems T7 (Promega). The bi-cistronic reporter RNAs (0.5 mg) were transfected using the TransIT mRNA transfection kit (Mirus Bio, Madison, WI, USA), following the manufacturer's protocol. The pRF-FMDV-IRES and pRF-CSF-IRES RNAs were synthesized using RiboMax large-scale RNA production systems (Promega Co.) with *Hpa*I digested plasmid DNAs.

For quantification of *PKD1L3* mRNA and *USP31* mRNA levels, we used specific primers; PKD1L3 sense 5′-TGTCATCCCATCAGCCAGTT-3′ and anti-sense 5′-TGTTTCTGCCAGAGATTGCC-3′, and USP31 sense USP31–700S:5′- TGT GGC TTT TGG ACC GAG TTGC-3′and USP31–900AS:5′- TGC AGT GAG AAC ATT TGC CTGC-3′, as described previously (Ide et al., 2022).

2.5. Virus replication and infection

We examined the effects of PKD1L3 and USP31 on CSFV replication, by transfecting cells with targeting siRNAs and rGPE-N^{pro}-Luc-IRES-NS3 RNA (Tamura et al., 2015), using a *Trans*IT-mRNA transfection Kit (Mirus Co.).

We also evaluated the effects of PKD1L3 and USP31 on EMCV virus (ATCC) infection, by siRNA transfection of HEK293 cells, as described above. siRNA-transfected cells were infected with EMCV at a multiplicity of infection (MOI)=0.1. Intracellular EMCV RNA was isolated using ISOGEN (Nippon Gene Co., Ltd., Tokyo, Japan) at 3 days post-infection, and subject to quantitation by qRT-PCR using primers (241S; 5′- AACGTCTGTAGCGACCCTTT-3′ and 409A, 5′-TACGCTTGAG-GAGAGCCATT-3′) and Brilliant III Ultra-Fast SYBR^s Green qRT-PCR master mix (Agilent Technologies, Santa Clara, CA, USA).

2.6. Plasmid construction and sequencing

We used pRF-EGFP-PURO-EF1A-hPKD1L3-Myc (Fig. 2A) and pRF-EGFP-PURO-EF1A-hUSP31-HA (Fig. 2B) plasmids, which had been constructed by a commercial supplier of customized gene vectors (VectorBuilder Inc., Kanagawa, Japan). DNA sequencing was commissioned to a specialist laboratory (Eurofins Japan, Tokyo, Japan). DNA sequence characterization was performed using GENETYX-Mac software

(GENETYX Co., Tokyo, Japan) and GENBANK.

2.7. Immunoprecipitation assay

HEK293 cells were transfected with pRF-EGFP-PURO-EF1A-hPKD1L3-Myc, pRF-EGFP-PURO-EF1A-hUSP31-HA, or vector DNA using the Lipofectamine™ LTX reagent (Thermo Fisher Scientific Inc.) and lysed with IP lysis buffer (Pierce Co.) with PhosStop (Sigma) and cOmplete™ ULTRA, EDTA-free, mini (Sigma) following the manufacturer's protocol. Anti-HA antibody (BioVision Research Products, California, USA) or anti-Myc antibody (MBL Co.) was conjugated to Magnosphere™ MS300/Carboxyl beads using (1-Ethyl-3-(3-dimethyla-minocopropyl) carbodiimide hydrochloride); EDC, 10 mg/mL), following the manufacturer's protocol. The Ab beads were reacted with the cell lysate, precipitated with a magnet, and washed with IP buffer. Specific bound proteins were eluted by using elution buffer (10 mM Tris pH 8, 300 mM NaCl, 5 mM EDTA pH 8, 1 % SDS) at 95 °C for 15 min. Bound proteins were analyzed by Western blot assay using specific antibodies, following the standard protocol (Ide et al., 2022).

2.8. Immunofluorescence assay

The cells were fixed with cold acetone-methanol at −30 °C for 10 min. The samples were then incubated with anti-PKD1L3 rabbit antibody (ab234670, Abcam Co., Cambridge, UK), anti-USP31 mouse monoclonal antibody (sc-100634, Santa Cruz Co.), anti-eIF3c rabbit antibody (ab237757, Abcam Co.), and anti-Hsp90 beta rabbit antibody (Ab2927, Abcam Co.). The primary antibodies were detected using anti-mouse Alexa 568 (Dako Co., Osaka, Japan) or anti-rabbit Alexa 488 antibodies (Dako Co.). The cells were observed using a BZ-X-700 microscope (Keyence Co., Osaka, Japan).

2.9. Statistical analysis

All data are presented as the mean ± standard deviation (S.D.) from three independent experiments. The figures were generated using GraphPad Prism (version 9) software. Statistical analysis was performed using Dunnett's multiple comparison tests to evaluate significant differences after One-way ANOVA analysis of variance. Statistical significance was set at $p < 0.1$ or 0.05.

3. Results

3.1. Effect of PKD1L3 and USP31 on FMDV- and CSFV-IRES

We had previously proposed PKD1L3 and USP31 as potential common host factors for IRES-mediated translation of mRNA for both FMDV and CSFV (Ide et al., 2022). To substantiate our previous findings, we conducted an RNA-silencing experiment to investigate relative IRES activities in mock-transfected cells versus bi-cistronic FL and RL reporter RNA with the FMDV- or CSFV- IRES transfected with the relevant siRNA
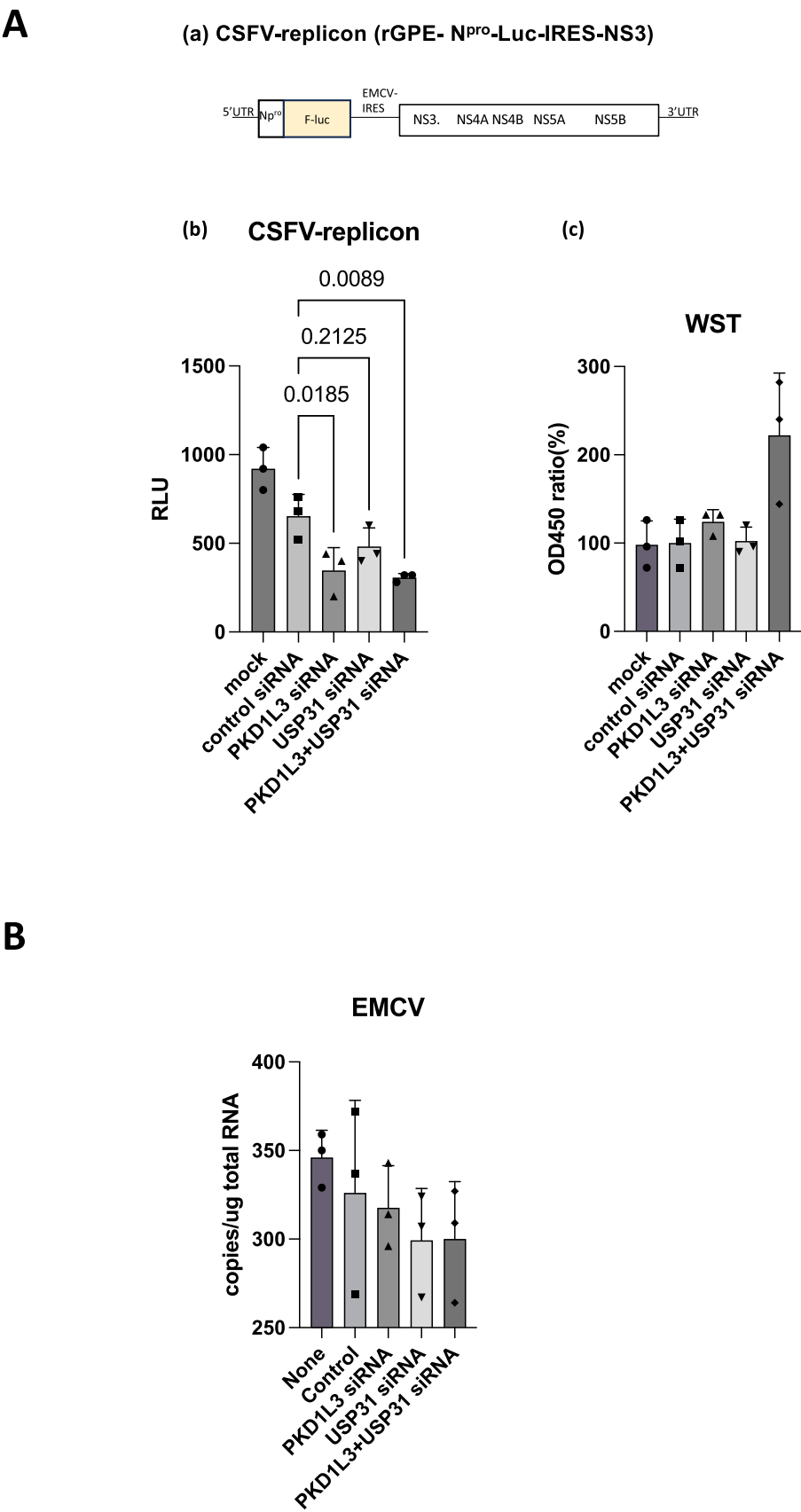
A

(a) CSFV-replicon (rGPE- N^pro-Luc-IRES-NS3)

(b) **CSFV-replicon** **(c)** **WST**

B

EMCV

Fig. 4. Roles of PKD1L3 and USP31 in viral replication. (**A**) Effects of *PKD1L3* and *USP31* siRNA treatment on CSFV replication. (**a**) The structure of the CSFV replicon, rGPE- N^pro-Luc-IRES-NS3. (**b**) Effects of *PKD1L3* and *USP31* siRNA treatment on the CSFV replicon. CSFV replication activity was measured based on firefly (F-luc) activity. (**c**) Effect of siRNA treatment on cell viability, as measured in a WST assay. (**B**) Effects of *PKD1L3* and *USP31* siRNA treatment on EMCV infection.
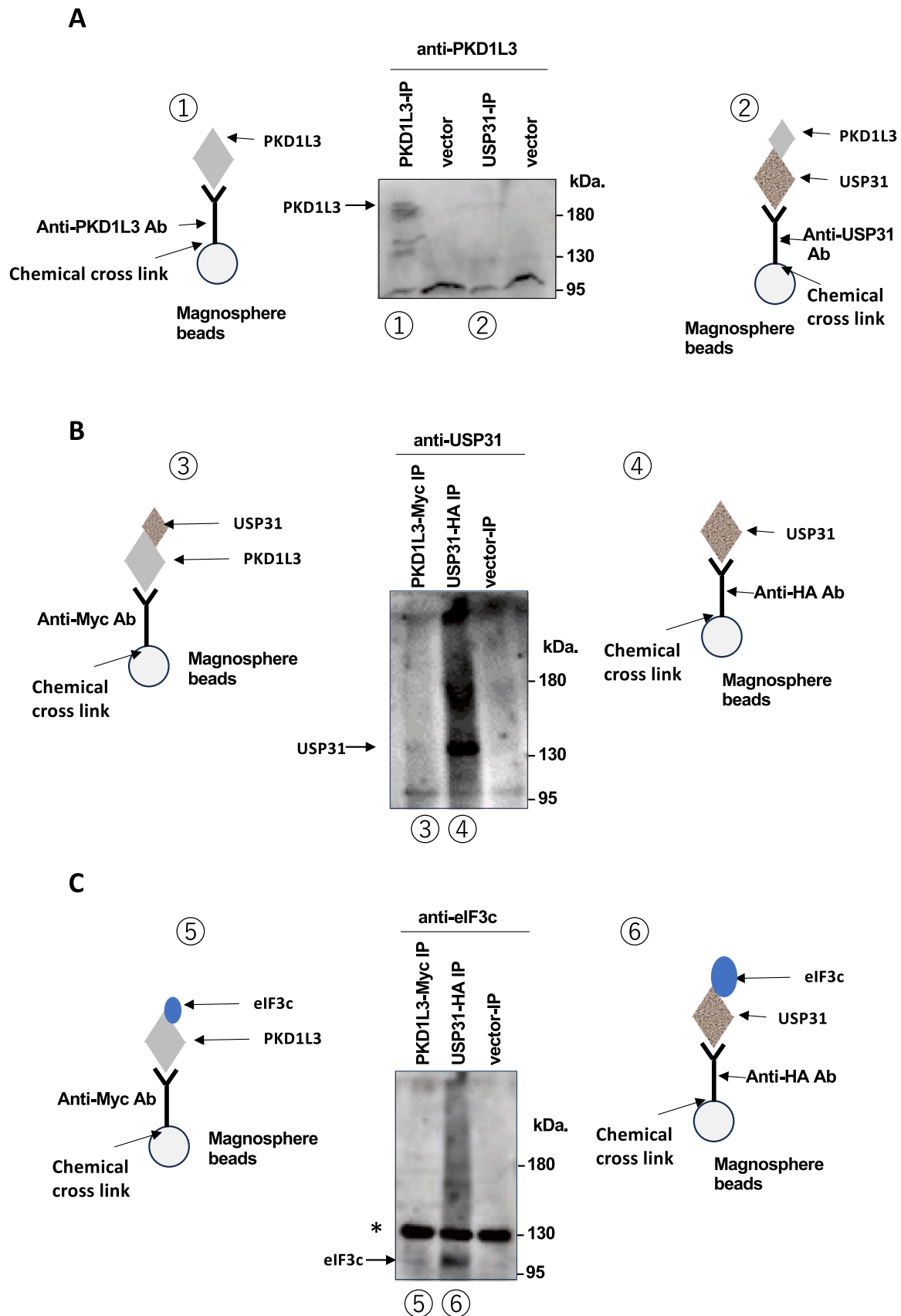
Fig. 5. Delineation of PKD1L3 and USP31 protein interactions. Schematic IP methods of PKD1L3 and USP31 interacting proteins using anti-HA or Myc Abs conjugated Magnosphere beads are shown in both sides. (**A**) HEK293 cells were transfected with pRF-EGFP-PURO-EF1A-hPKD1L3-Myc, pRF-EGFP-PURO-EF1A-hUSP31-HA, or control expression vectors (pRF-EGFP-PURO) plasmid DNAs. Cell lysates (400 mg/reaction) were precipitated with anti-PKD1L3 (①) and anti-USP31 (②) antibodies conjugated beads, respectively, and then subjected to a Western blot assay using anti-PKD1L3 Ab (Abcam). PKD1L3 and molecular weight markers are

indicated. (**B**) PKD1L3, USP31 expression vectors, and control vector were transfected and immunoprecipitated by anti-Myc (③) and anti-HA (④) antibodies conjugated beads and reacted with anti-USP31 Ab (Santa Cruz). USP31 and molecular weight markers are indicated. (**C**) PKD1L3 and USP31 expression and control vectors were transfected and immunoprecipitated by anti-Myc Ab (⑤) and anti-HA Ab (⑥) conjugated beads, respectively. Transferred IP proteins were reacted with anti-eIF3c Ab. eIF3c and molecular weight markers are indicated. *Immunoglobulin monomer. (**D**) Detection of myc-PKD1L3, PKD1L3, HA-USP31, USP31, eIF3c, and actin in cell lysates (40 mg/lane) by WB analysis.
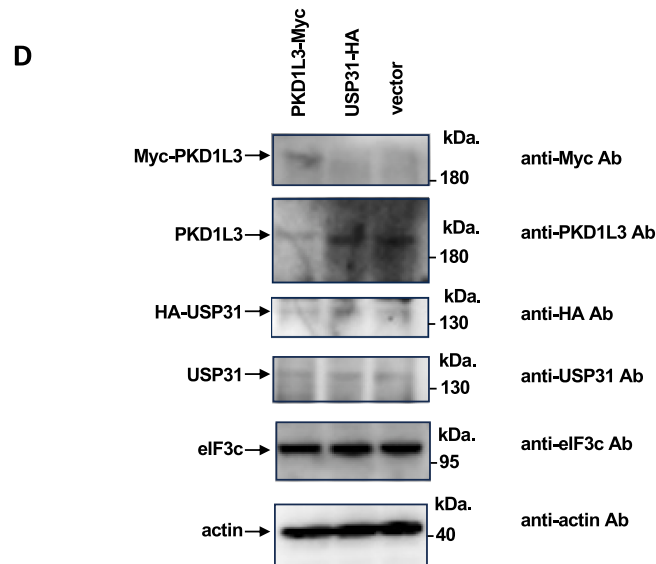
Fig. 5. (*continued*).

or control siRNA. The bi-cistronic reporter RNAs were synthesized from plasmids (Supplementary Fig.S2) and transfected into cells as described in Materials and Methods. Silencing *PKD1L3* or both *PKD1L3* and *USP31* significantly suppressed relative FMDV- and CSFV-IRES activities, without producing significant cytotoxicity (Figs. 1A, B, S3). We also found that silencing *USP31* also significantly lowered relative IRES activity for CSFV, although the reduction was less pronounced than that produced by silencing *PKD1L3* or both *PKD1L3* and *USP31*. We evaluated the effects of *PKD1L3* siRNA and *USP31* siRNA in qRT-PCR assays and found specific and significant suppression of both genes' expression (Fig. 1C). Our findings thus indicate that PKD1L3 and USP31 are common host factors exploited by both the FMVD- and CSFV-IRESes to propagate in host cells.

We then constructed the pRF-EGFP-PURO-EF1A-hPKD1L3-Myc and pRF-EGFP-PURO-EF1A-hUSP31-HA vectors to investigate how PKD1L3 and USP31 overexpression affects IRES activity (Fig. 2A, B). We also confirmed that the Enhanced Green Fluorescent Protein (EGFP), PKD1L3, and USP31 expression in these plasmids partially merged in the cytoplasm (Fig. 2C, D, yellow color).

Experiments with these plasmid vectors revealed that PKD1L3 and USP31 overexpression (0.3, 1.0 mg/plasmid DNA) did not significantly affect IRES activity or cell viability versus vector plasmid controls using bi-cistronic reporter RNA (Fig. 3A, B). Furthermore, we also found no effect of PKD1L3 or USP31 overexpression in our FMDV-IRES-expressing cell line (B10) or our CSFV-IRES-expressing cell line (pCI5) (Ide et al., 2022), as determined from the absence of significant changes in the IRES activity and cell viability (Fig. 3C, D).

3.2. Roles of PKD1L3 and USP31 in viral replication

To further examine the roles of PKD1L3 and USP31 in viral replication, we examined the effects of their silencing. We first examined the effects of *PKD1L3* and *USP31* siRNAs on CSFV replication (Fig. 4A). Silencing of *PKD1L3,* and silencing of both *PKD1L3* and *USP31,* significantly suppressed CSFV replication (Fig. 4A-a, b) without cytotoxicity (Fig. 4A-c). We next examined the roles of PKD1L3 and USP31 in picornavirus infection (Fig. 4B). We selected EMCV as it belongs to the same family as FMDV (*picornaviridae*), and possesses an IRES. We found

that silencing of *USP31,* and silencing of both *PKD1L3* and *USP31,* decreased EMCV RNA level at 3 days post-infection (Fig. 4B).

3.3. PKD1L3 and USP31 interaction with eIF3c and HSP90β

To clarify the roles of PKD1L3 and USP31 in IRES-mediated translation, we examined the interactions between PKD1L3, USP31, and other proteins of interest—specifically, the translation factor eukaryotic translation initiation factor 3 subunit c (eIF3c) and its chaperone, heat shock protein HSP90-beta (Hsp90β), which are reportedly involved in HCV-IRES functions (Ujino et al., 2012), in immunoprecipitation assays. That report highlighted the indirect, HCV-IRES RNA-mediated binding of Hsp90 to the eIF3c subunit, and the consequent abolition of subunit ubiquitination and proteasome-dependent degradation and showed that the knockdown of *eIF3c* resulted in an inhibitory effect on the translation of HCV-derived RNA. The CSFV-IRES shows high structural and sequential similarity to the HCV-IRES, and it reportedly binds eIF3c (Erzberger et al., 2014; Hashem et al., 2013; Yamamoto, Unbehaun and Spahn, 2017). The FMDV-IRES has also previously been reported to interact with eIF3c (Lopez de Quinto, Lafuente and Martinez-Salas, 2001; Pilipenko et al., 2000). Interestingly, a recent study indicated that USP31 reduces Hsp90β ubiquitination, resulting in increased Hsp90β levels in a nonalcoholic steatohepatitis (NASH) mouse model (Zhang et al., 2024). Therefore, we hypothesized that Hsp90 would be involved in CSFV-IRES and FMDV-IRES activities in association with eIF3c, and that both these proteins would interact with common host factors PKD1L3 and USP31.

We first fixed anti-PKD1L3 or USP31 antibodies (Fig. 5A) and anti-Myc or anti-HA antibodies (Fig. 5B) to Magnosphere™ gel to examine the interaction between PKD1L3 and USP31. USP31 was less strongly precipitated by PKD1L3 than PKD1L3 itself (Fig. 5A, B), indicating a potential interaction between these two factors, which is weaker than self-interaction. After precipitation of PKD1L3 with an anti-Myc antibody and USP31 with an anti-HA antibody, their interactions with eIF3c were examined by immunoblotting using an anti-eIF3c antibody (Fig. 5C). We obtained strong detection for eIF3c after precipitation with recombinant USP31 using anti-HA Ab (Fig. 5C⑥). Anti-Myc Ab-mediated recombinant PKD1L3 precipitation yielded less pronounced eIF3c
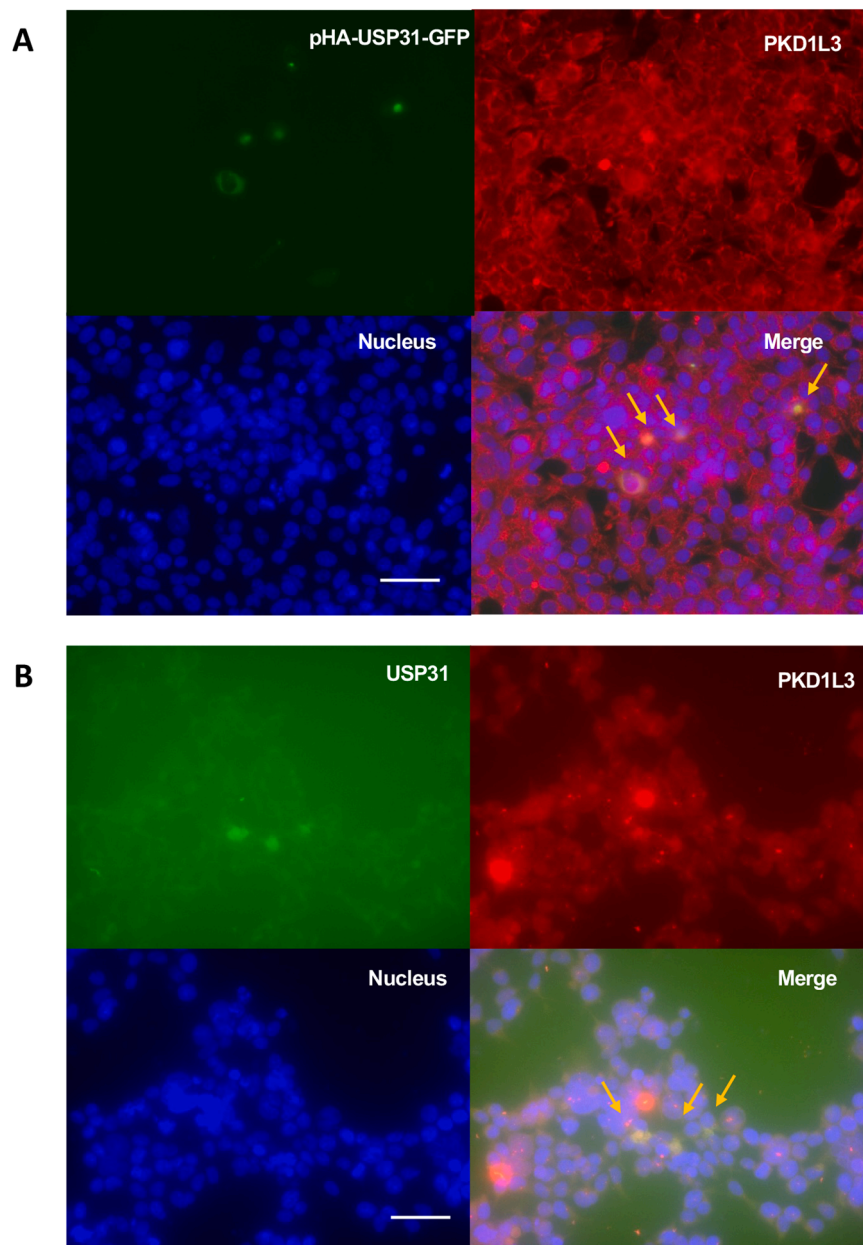
Fig. 6. Localization of PKD1L3 and USP31 in cells. (**A**) HEK293 cells were transfected with pRF-EGFP-PURO-EF1A-hPKD1L3-Myc plasmid DNA and stained with anti-PKD1L3 antibody. EGFP, anti-PKD1L3 and anti-rabbit Alexa 568, DAPI staining, and the merged image was shown. HEK293 cells were also reacted with anti-PKD1L3 and anti-USP31 (**B**), anti-eIF3c and anti-USP31 antibodies (**C**), anti-Hsp90 and anti-USP31 antibodies (**D**), and normal mouse and rabbit IgGs (**E**) using Alexa-488 and Alexa-568 conjugated second antibodies. A fluorescent microscope, BZ-X700 (Keyence Co., Japan) (x400), was used. The nucleus was stained with DAPI, and merged images are shown (merged signal is pointed by yellow arrows). The scale bars indicate 50 μm. The z-stack is 0.3 μm.

detection (Fig. 5C⑤). Therefore, eIF3c can be seen as interacting more strongly with USP31 than PKD1L3. The input of proteins into each prepared lysate is shown in Fig. 5D.

In order to further investigate the interactions between these proteins, we characterized the intracellular localizations of PKD1L3, USP31, eIF3c, and Hsp90β in an immunofluorescence assay (Fig. 6). We observed partial co-localization of PKD1L3 and USP31 in the cytoplasm using a USP31 expression vector (Fig. 6A) and antibody detection (Fig. 6A, B). We also observed partial co-localizations of eIF3c and USP31 (Fig. 6C), and of Hsp90β and USP31 (Fig. 6D) in the cytoplasm.

3.4. Roles of eIF3c and HSP90β in FMDV- and CSFV- IRESes

To investigate how eIF3c and Hsp90β participate in FMDV- and CSFV- IRES activities, we performed siRNA-mediated silencing experiments in our respective dedicated HEK293-based (B10 and pCI5) cell lines. Upon *eIF3c* and *Hsp90β* siRNA treatment, we observed significant reductions in both FMDV- and CSFV- IRES activities ($p < 0.1$ and 0.05, respectively) without any significant cytotoxicity (Fig. 7A, B). We then confirmed these silencing effects using *eIF3c*- and *Hsp90*-targeting siRNAs in a Western blot assay (Fig. 7C).
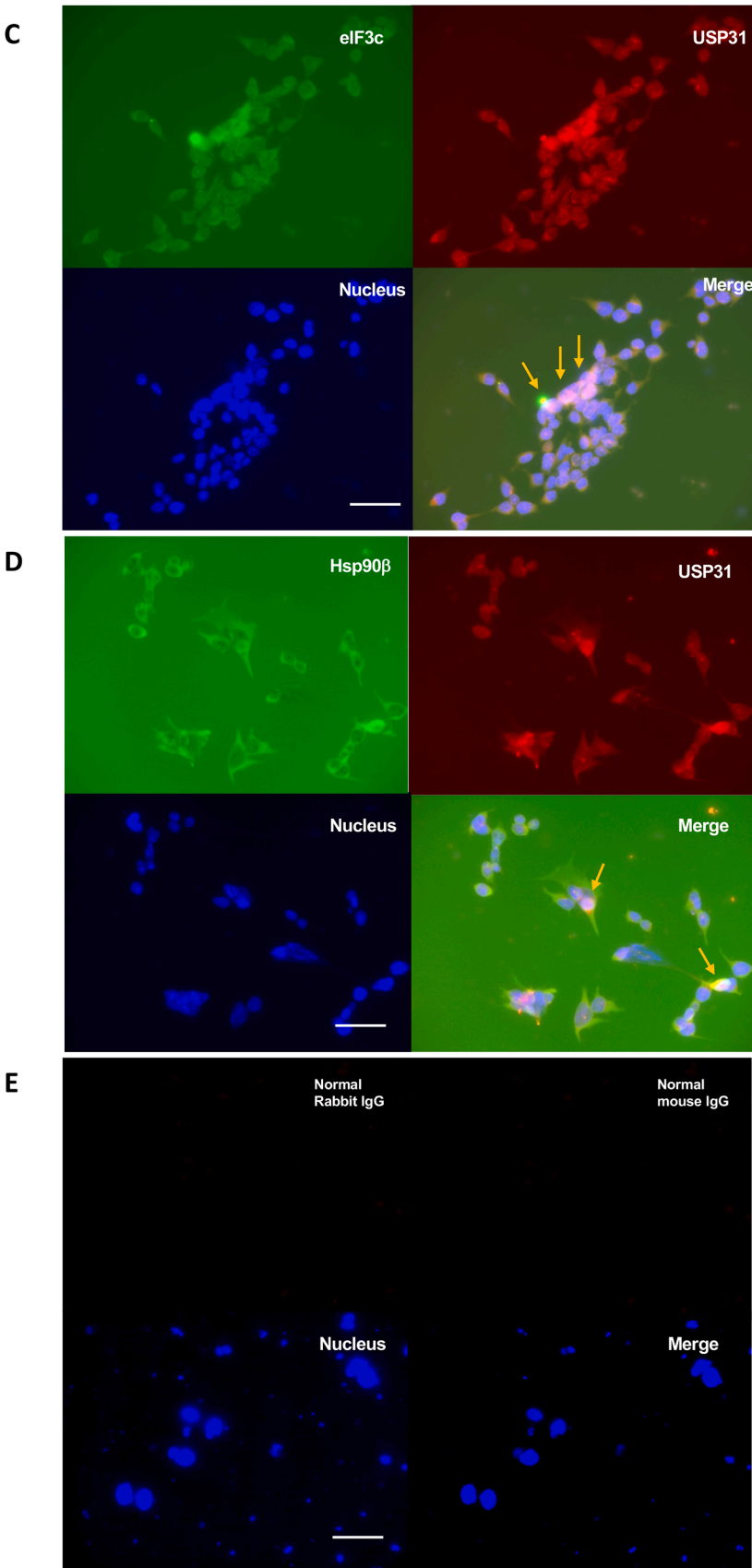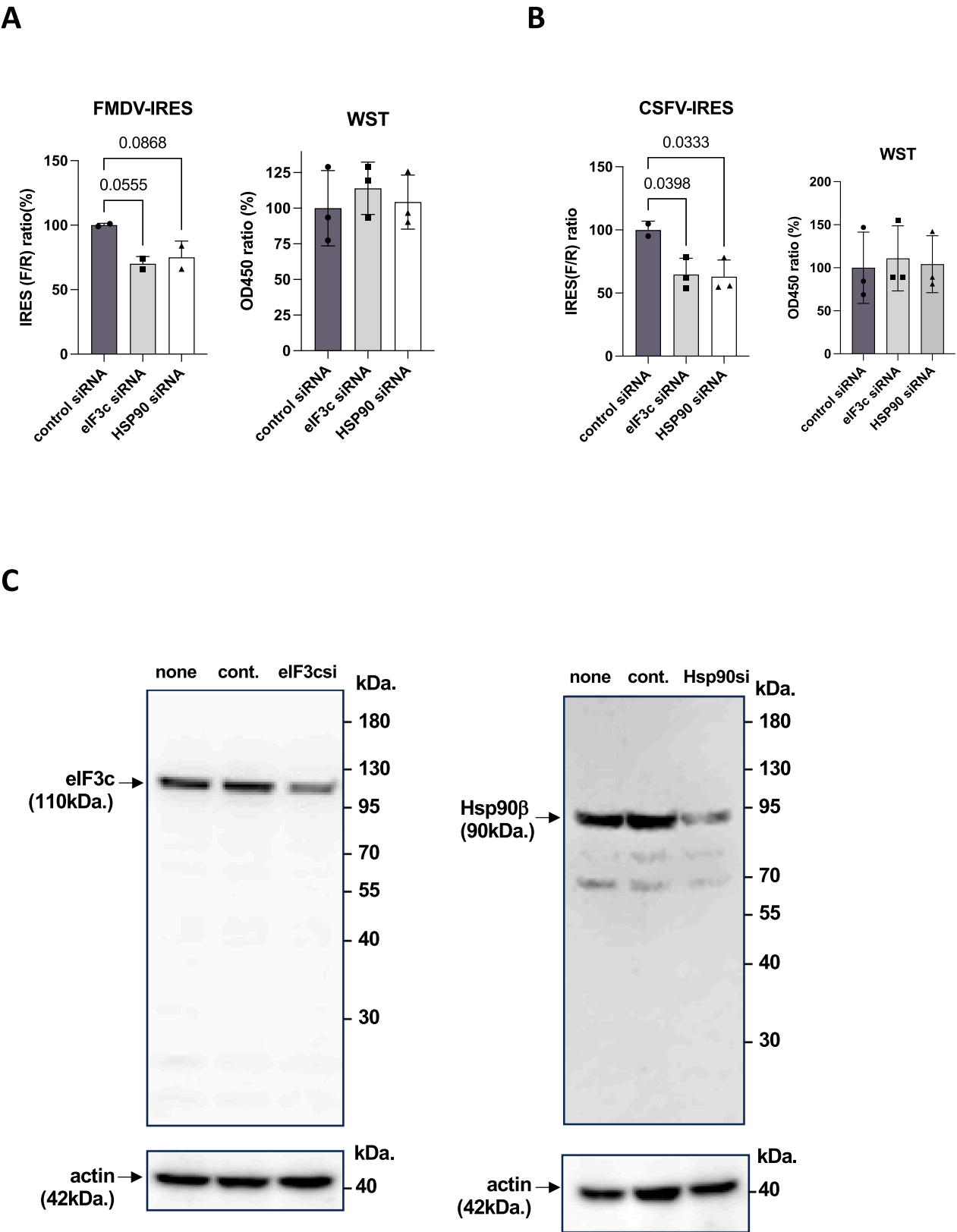
Fig. 6. (*continued*).

Fig. 7. eIF3c and Hsp90β involvement in IRES activities. (**A**) Silencing of *eIF3c* and *Hsp90β* in B10 (FMDV-IRES) and (**B**) pCI5 (CSFV-IRES) cells (left). Cell viability was determined in a WST-1 assay (**A, B**, right). The percentage of F/R or OD_{450} value of each siRNA treated cells when compared to the control siRNA-treated cells is indicated. Vertical bars represent SD. Significant suppressions less than $p = 0.1$ was shown. (**C**) Silencing of *eIF3c* and *Hsp90β* was confirmed by WB analysis. B10 cells treated with control siRNA and *eIF3c* siRNA or *Hsp90β* siRNA was examined with specific antibodies. Actin was detected as an internal control.

4. Discussion

We aimed to confirm the roles of PKD1L3 and USP31 as common host factors in IRES-mediated RNA translation for FMDV and CSFV, and to investigate the roles of these factors in viral replication and infection by elucidating their interactions with each other and with other host proteins. To the authors' knowledge, this is the first such detailed report on the exploitation of these host factors by two viruses belonging to different families and possessing different types of IRES.

In the first key findings in this study, we established that PKD1L3 and USP31 are both host factors exploited by the IRES mechanism for the translation of FMDV and CSFV RNA, based on bi-cistronic reporter assays. Silencing of PKD1L3 and USP31 significantly suppressed FMDV- and CSFV- activities in these assays, demonstrating these factors are required for the viruses to invade host cells. These findings are consistent with our previous results in IRES-expressing cells (Ide et al., 2022), and we also found that PKD1L3 appears to play a more pronounced IRES-related role than USP31, which is also consistent with the results of microarray analysis in our previous study (Ide et al., 2022). Furthermore, in northern blot analysis, we were able to confirm that the FMDV-IRES bi-cistronic DNA vector did not contain a cryptic promoter in its genome, as the expected size of a single band was detected in FMDV-IRES vector-containing cell lines (Matsui et al., 2019). Excluding the possibility of cryptic promoters by using bi-cistronic reporter plasmid DNA allows us to rule out any possible unintended RNA generation that could compromise the measurement of IRES activity.

In further assays with pRF expression vectors, we found no significant effect on IRES activity following exogenous overexpression of PKD1L3 or USP31. Therefore, we consider that PKD1L3 and USP31 may reach a saturation point for intracellular FMDV-IRES and CSFV-IRES activities.

We also confirmed that the silencing of *PKD1L3* and *USP31* can suppress CSFV replication and prevent EMCV infection (the latter is a picornavirus, and thus belongs to the same family as FMDV), and we consider these findings may reflect the suppression of IRES activities for these two viruses.

Our study provides some evidence on the roles that PKD1L3 and USP31 play in viral RNA translation, based on investigations of their mutual interaction and their interactions with other factors. PKD1L3 and USP31 demonstrated weak, mutual precipitation in immunoprecipitation assays, and cytoplasmic co-localization in immunofluorescence assays. We targeted the translation factor, eIF3c, which is reportedly involved in HCV-IRES function (Hashem et al., 2013; Zhou et al., 2008) and has Hsp90β as its chaperone (Ujino et al., 2012) (Fig. 4C). We found cytoplasmic co-localization for eIF3c and Hsp90β with USP31, results which are consistent with a previous report that Hsp90β interacts with USP31 (Zhang et al., 2024).

Understanding how these host factors interact with a virus IRES may involve a consideration of their normal biological functions. PKD1L3 forms a complex with the polycystic TRP subfamily member PKD2L1, which is involved in physiological responses to diverse stimuli via Ca^{2+} influx and entry (Hu et al., 2015). PKD1L3 and PKD2L1 are also candidate receptors for sour taste (Huang et al., 2006; Ishimaru et al., 2006), although *PKD1L3*-mutant mice reportedly show no defects in taste reception (Nelson et al., 2010). *PKD1L3* belongs to the family of *pkd* genes that have been reported to regulate zebrafish development (England et al., 2017), and polycystin-1, encoded by the PKD1 gene, regulates the microtubular cytoskeleton to modulate cell adhesion and migration (Castelli et al., 2015). USP31 belongs to a large family of cysteine proteases that function as deubiquitinating enzymes (Tzimas et al., 2006) and localize to postsynaptic lipid rafts (Tian et al., 2003). USP31 reportedly regulates NF-κB and tumor progression (Hou et al., 2021; Huang et al., 2023; Ye et al., 2018). However, the detailed PKD1L3- and USP31-regulated IRES-related effector mechanisms remain elusive.

Of the other host proteins we investigated in this study, eIF3 is a vital translation initiation factor which reportedly allows the HCV-IRES to gain access to the 40S subunit (Hashem et al., 2013), and is composed of 13 subunit complexes (Zhou et al., 2008). Among eIF3 subunits, it has been reported that the helix loop-helix motif in eIF3c subunit is highly conserved in all eukaryotes and may have a universal role in eukaryotic translation initiation (Sun et al., 2013). eIF3c reportedly interacts with Hsp90 via HCV-IRES RNA (Ujino et al., 2012). A recent study indicated that USP31 reduces Hsp90β ubiquitination, resulting in increased Hsp90β levels in a nonalcoholic steatohepatitis (NASH) mouse model (Zhang et al., 2024).

Considering what is known about the functional relationships between these proteins, the results of this study suggest that PKD1L3 and USP31 interact with eIF3c and Hsp90β to maintain FMDV- and CSFV-IRES activities. A previous cryoelectronic microscopy study highlighted the possibility that eIF3 is displaced from its ribosomal position in the 43S complex through interaction with the CSFV-IRES (Hashem et al., 2013). Such displacement may prevent the formation of the 43S complex and favor the translation of viral mRNA. eIF3c reportedly plays a primary role in 40S ribosome subunit binding and exchanges eIF5B with eIF2 after start codon recognition (Sun et al., 2013). Therefore, PKD1L3 and USP31 may participate in this regulation through eIF3c, as we demonstrated that PKD1L3 can interact directly and/or indirectly with eIF3c through USP31. The participation of eIF3c and Hsp90b in FMDV- and CSFV-IRES activities was also demonstrated in this study (Fig. 6C).

In conclusion, this study establishes PKD1L3 and USP31 as common host factors exploited in IRES-mediated RNA translation by FMDV and CSFV. It also provides the first report on PKD1L3 and USP31 interactions with eIF3c and Hsp90β, which may also play a role in such viral IRES-mediated translation. Our results may support future research initiatives, such as *in vivo* testing in *PKD1L3* and *USP31*-knockout mice as a step toward future establishment of disease-resistant livestock in strategies to combat FMDV and CSFV. Furthermore, these results may benefit research on a range of other viruses that rely on IRES-mediated translation to infect their hosts.

Ethics approval

This study was performed in accordance with the plan of the recombinant DNA experiment on "Analysis of IRES dependent translation mechanism *in vivo*", which was approved by the Recombinant DNA or Animal Experiment Committee of Kagoshima University (Approval No. K28017, VM23004).

Author statements

None.

Ethics approval

This study was performed in accordance with the plan of the recombinant DNA experiment on "Analysis of IRES dependent translation mechanism *in vivo*", which was approved by the Recombinant DNA or Animal Experiment Committee of Kagoshima University (ApprovalNo. K28017, VM23004).

Consent for publication

All authors give consent for the publication of this study.

Author agreement

All authors agree with the inclusion of Dr Yoshihiro Sakoda as a co-author for revision.

CRediT authorship contribution statement

Rupaly Akhter: Writing – original draft, Visualization, Validation, Methodology, Investigation, Formal analysis, Data curation. **Kazi Anowar Hossain:** Methodology, Investigation, Data curation. **Bouchra Kitab:** Writing – review & editing, Methodology, Data curation, Conceptualization. **Yoshihiro Sakoda:** Resources, Data curation. **Kyoko Tsukiyama-Kohara:** Writing – review & editing, Writing – original draft, Supervision, Investigation, Funding acquisition, Data curation, Conceptualization.

Declaration of competing interest

The authors declare no conflict of interest.

Supplementary materials

Supplementary material associated with this article can be found, in the online version, at doi:10.1016/j.virusres.2025.199570.

Data availability

The datasets analyzed in the current study are available from the corresponding author upon reasonable request.

References

Belsham, G.J., Brangwyn, J.K., 1990. A region of the 5′ noncoding region of foot-and-mouth disease virus RNA directs efficient internal initiation of protein synthesis within cells: involvement with the role of L protease in translational control. J. Virol. 64, 5389–5395.

Castelli, M., De Pascalis, C., Distefano, G., Ducano, N., Oldani, A., Lanzetti, L., Boletta, A., 2015. Regulation of the microtubular cytoskeleton by Polycystin-1 favors focal adhesions turnover to modulate cell adhesion and migration. BMC Cell Biol. 16, 15.

England, S.J., Campbell, P.C., Banerjee, S., Swanson, A.J., Lewis, K.E., 2017. Identification and expression analysis of the complete Family of Zebrafish pkd genes. Front. Cell Dev. Biol. 5, 5.

Erzberger, J.P., Stengel, F., Pellarin, R., Zhang, S., Schaefer, T., Aylett, C.H.S., Cimermancic, P., Boehringer, D., Sali, A., Aebersold, R., Ban, N., 2014. Molecular architecture of the 40S eIF1 eIF3 translation initiation complex. Cell 158, 1123–1135.

Grubman, M.J., Baxt, B., 2004. Foot-and-mouth disease. Clin. Microbiol. Rev. 17, 465–493.

Hashem, Y., des Georges, A., Dhote, V., Langlois, R., Liao, H.Y., Grassucci, R.A., Pestova, T.V., Hellen, C.U., Frank, J., 2013. Hepatitis-C-virus-like internal ribosome entry sites displace eIF3 to gain access to the 40S subunit. Nature 503, 539–543.

Hossain, K.A., Akhter, R., Rashid, M.H.O., Akter, L., Utsunomiya, M., Kitab, B., Ngwe Tun, M.M., Hishiki, T., Kohara, M., Morita, K., Tsukiyama-Kohara, K., 2024. Suppression of dengue virus replication by the French maritime pine extract pycnogenol(R). Virus Res. 339, 199244.

Hou, Y., Fan, Y., Xia, X., Pan, J., Hou, J., Liu, X., Chen, X., 2021. USP31 acetylation at Lys1264 is essential for its activity and cervical cancer cell growth. Acta Biochim. Biophys. Sin. 53, 1037–1043 (Shanghai).

Hu, M., Liu, Y., Wu, J., Liu, X., 2015. Influx-operated Ca(2+) entry via PKD2-L1 and PKD1-L3 channels facilitates sensory responses to polymodal transient stimuli. Cell Rep. 13, 798–811.

Huang, A.L., Chen, X., Hoon, M.A., Chandrashekar, J., Guo, W., Trankner, D., Ryba, N.J., Zuker, C.S., 2006. The cells and logic for mammalian sour taste detection. Nature 442, 934–938.

Huang, Y., Jiang, P., Chen, Y., Wang, J., Yuan, R., 2023. Systemic analysis of the expression and prognostic significance of USP31 in endometrial cancer. Biomol. Biomed. 23, 426–436.

Ide, Y., Kitab, B., Ito, N., Okamoto, R., Tamura, Y., Matsui, T., Sakoda, Y., Tsukiyama-Kohara, K., 2022. Characterization of host factors associated with the internal ribosomal entry sites of foot-and-mouth disease and classical swine fever viruses. Sci. Rep. 12, 6709.

Ishimaru, Y., Inada, H., Kubota, M., Zhuang, H., Tominaga, M., Matsunami, H., 2006. Transient receptor potential family members PKD1L3 and PKD2L1 form a candidate sour taste receptor. Proc. Natl. Acad. Sci. U. S. A. 103, 12569–12574.

Jackson, R.J., Kaminski, A., 1995. Internal initiation of translation in eukaryotes: the picornavirus paradigm and beyond. RNa 1, 985–1000.

Jamal, S.M., Belsham, G.J., 2013. Foot-and-mouth disease: past, present and future. Vet. Res. 44, 116.

Jang, S.K., Davies, M.V., Kaufman, R.J., Wimmer, E., 1989. Initiation of protein synthesis by internal entry of ribosomes into the 5′ nontranslated region of encephalomyocarditis virus RNA *in vivo*. J. Virol. 63, 1651–1660.

Kanda, T., Ozawa, M., Tsukiyama-Kohara, K., 2016. IRES-mediated translation of foot-and-mouth disease virus (FMDV) in cultured cells derived from FMDV-susceptible and -insusceptible animals. BMC Vet. Res. 12, 66.

Lopez de Quinto, S., Lafuente, E., Martinez-Salas, E., 2001. IRES interaction with translation initiation factors: functional characterization of novel RNA contacts with eIF3, eIF4B, and eIF4GII. RNa 7, 1213–1226.

Lozano, G., Martinez-Salas, E., 2015. Structural insights into viral IRES-dependent translation mechanisms. Curr. Opin. Virol. 12, 113–120.

Matsui, T., Handa, Y., Kanda, T., Tsukiyama-Kohara, K., 2019. Silencing of the foot-and-mouth disease virus internal ribosomal entry site by targeting relatively conserved region among serotypes. Virus Genes 55, 786–794.

Nelson, T.M., Lopezjimenez, N.D., Tessarollo, L., Inoue, M., Bachmanov, A.A., Sullivan, S.L., 2010. Taste function in mice with a targeted mutation of the pkd1l3 gene. Chem. Senses 35, 565–577.

Pilipenko, E.V., Pestova, T.V., Kolupaeva, V.G., Khitrina, E.V., Poperechnaya, A.N., Agol, V.I., Hellen, C.U., 2000. A cell cycle-dependent protein serves as a template-specific translation initiation factor. Genes Dev. 14, 2028–2045.

Rijnbrand, R., van der Straaten, T., van Rijn, P.A., Spaan, W.J., Bredenbeek, P.J., 1997. Internal entry of ribosomes is directed by the 5′ noncoding region of classical swine fever virus and is dependent on the presence of an RNA pseudoknot upstream of the initiation codon. J. Virol. 71, 451–457.

Sun, C., Querol-Audi, J., Mortimer, S.A., Arias-Palomo, E., Doudna, J.A., Nogales, E., Cate, J.H., 2013. Two RNA-binding motifs in eIF3 direct HCV IRES-dependent translation. Nucleic Acids Res. 41, 7512–7521.

Tamura, T., Ruggli, N., Nagashima, N., Okamatsu, M., Igarashi, M., Mine, J., Hofmann, M.A., Liniger, M., Summerfield, A., Kida, H., Sakoda, Y., 2015. Intracellular membrane association of the N-terminal domain of classical swine fever virus NS4B determines viral genome replication and virulence. J. Gen. Virol. 96, 2623–2635.

Tian, Q.B., Okano, A., Nakayama, K., Miyazawa, S., Endo, S., Suzuki, T., 2003. A novel ubiquitin-specific protease, synUSP, is localized at the post-synaptic density and post-synaptic lipid raft. J. Neurochem. 87, 665–675.

Tsukiyama-Kohara, K., Iizuka, N., Kohara, M., Nomoto, A., 1992. Internal ribosome entry site within hepatitis C virus RNA. J. Virol. 66, 1476–1483.

Tzimas, C., Michailidou, G., Arsenakis, M., Kieff, E., Mosialos, G., Hatzivassiliou, E.G., 2006. Human ubiquitin specific protease 31 is a deubiquitinating enzyme implicated in activation of nuclear factor-kappaB. Cell Signal. 18, 83–92.

Ujino, S., Nishitsuji, H., Sugiyama, R., Suzuki, H., Hishiki, T., Sugiyama, K., Shimotohno, K., Takaku, H., 2012. The interaction between human initiation factor eIF3 subunit c and heat-shock protein 90: a necessary factor for translation mediated by the hepatitis C virus internal ribosome entry site. Virus Res. 163, 390–395.

van den Akker, G.G.H., Zacchini, F., Housmans, B.A.C., van der Vloet, L., Caron, M.M.J., Montanaro, L., Welting, T.J.M., 2021. Current practice in bicistronic IRES reporter use: a systematic review. Int. J. Mol. Sci. 22.

Yamamoto, H., Unbehaun, A., Spahn, C.M.T., 2017. Ribosomal chamber music: toward an understanding of IRES mechanisms. Trends Biochem. Sci. 42, 655–668.

Ye, S., Lawlor, M.A., Rivera-Reyes, A., Egolf, S., Chor, S., Pak, K., Ciotti, G.E., Lee, A.C., Marino, G.E., Shah, J., Niedzwicki, D., Weber, K., Park, P.M.C., Alam, M.Z., Grazioli, A., Haldar, M., Xu, M., Perry, J.A., Qi, J., Eisinger-Mathason, T.S.K., 2018. YAP1-Mediated suppression of USP31 enhances NFkappaB activity to promote sarcomagenesis. Cancer Res. 78, 2705–2720.

Zhang, W., Lu, J., Feng, L., Xue, H., Shen, S., Lai, S., Li, P., Li, P., Kuang, J., Yang, Z., Xu, L., 2024. Sonic hedgehog-heat shock protein 90beta axis promotes the development of nonalcoholic steatohepatitis in mice. Nat. Commun. 15, 1280.

Zhou, M., Sandercock, A.M., Fraser, C.S., Ridlova, G., Stephens, E., Schenauer, M.R., Yokoi-Fong, T., Barsky, D., Leary, J.A., Hershey, J.W., Doudna, J.A., Robinson, C.V., 2008. Mass spectrometry reveals modularity and a complete subunit interaction map of the eukaryotic translation factor eIF3. Proc. Natl. Acad. Sci. U. S. A. 105, 18139–18144.